ELSEVIER

Journal of Nuclear Materials 241–243 (1997) 873–877

journal of nuclear materials

Radial distributions and poloidal asymmetries of T-10 SOL parameters and turbulence

V.A. Vershkov *, S.A. Grashin, V.V. Dreval, V.V. Piterskii, S.V. Soldatov, A.N. Jakovets

Russian Research Center "Kurchatov Institute", Institute of Nuclear Fusion, Moscow 123182, Russia

Abstract

This work presents the results of T-10 SOL investigations with multipin Langmuir probes and correlation reflectometry. A special regime with a rail limiter deeply introduced from the bottom of the machine at SOL temperatures of up to 50 eV has been studied. Five types of plasma small scale turbulence were observed in the SOL, including the three previously found types of core turbulence. It was shown that the main SOL parameters are poloidally uniform. A high poloidal asymmetry of the fluctuations and the turbulent flux of particles, was found.

Keywords: Tokamak; SOL; Turbulence; Langmuir probes; Reflectometry; T-10; SOL plasma

1. Introduction

Three types of core turbulence were distinguished previously with correlation reflectometry [1,2]. The main goal of this paper was to compare the properties of the SOL and core turbulence. On the other hand, the use of Langmuir probes may give much more information about potential fluctuations and particle fluxes with a high time and space resolution. Thus, another goal was to investigate the SOL with the parameters close to the core ones and avoid the influence of the wall by means of deeply introduced rail limiter.

2. Experiment

The T-10 rail limiter was at a minor radius of 22 cm, while a circular carbon limiter at 33 cm and the wall at 38 cm. The major plasma radius was 1.5 m, a plasma current of 200 kA, a magnetic field of 2.65 T and an average density $2.5–2.7 \times 10^{19}$ m^{-3}. The influence of the magnetic gradient drift direction was checked by the toroidal field reversal. The turbulent density fluctuations in T-10 SOL were investigated with the help of a 7 pins Langmuir probe placed in the same port as the rail limiter and a set of Langmuir probes flush-mounted near the rail limiter tip. The magnetic field line from the probe can hit the rail limiter at least after two turns around the major axis of the tokamak in both directions. The two positions at low and high field side were used in the experiment. Two channels of T-10 three wave O-mode correlation reflectometer [3] or multipin probe were registered in each discharge at 1 MHz sampling rate.

3. Results

Radial profiles of density, temperature and floating potential of the SOL are presented in Fig. 1a–c. The symbols of different shape correspond to the high and low field side probe positions. The open and filled symbols are used for the up and down directions of the ion drift due to the gradient of magnetic field. In all four cases no systematic difference is observed within the scatter of experimental points, suggesting a high degree of symmetry in the SOL parameters. The floating potential is positive and reverses the sign near the rail limiter tip. The significant scatter of the floating potential is seen at $r \leq 26$ cm. The two dashed lines approximate the highest and lowest possible values.

The variation of the fluctuations characteristics with radius may be seen in Fig. 2. The ion saturation current of

* Corresponding author. Fax: +7-095 943 0073; e-mail: vershkov@qq.nfi.kiae.su.

PII S0022-3115(96)00623-X

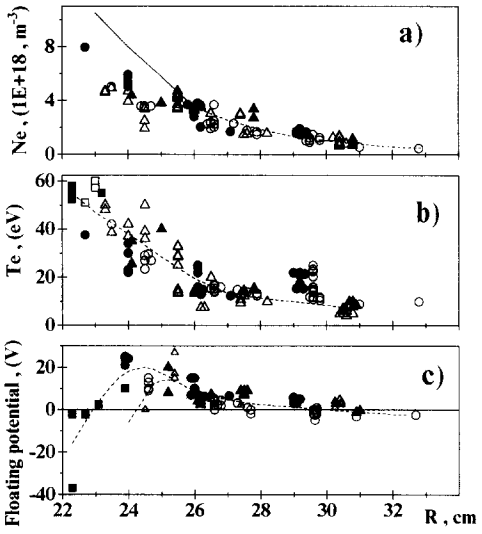

Fig. 1. Radial dependence of electron density (a); electron temperature (b) and floating potential (c). Filled triangles – low field side probe position, ion drift down; open triangles – low field side probe position, ion drift up; filled circles – high field side probe position, ion drift down; open circles – high field side probe position, ion drift up; filled squares – rail limiter probe, ion drift down; open squares – rail limiter probe, ion drift up; solid line – multichannel Interferometry data; dashed curves – approximation of the experimental data (two curves in Fig. 2c show the range of uncertainty in experimental data).

the two probes spaced poloidally 0.6 cm apart was measured in five radial positions of the probe on the low field side. Fig. 2f presents the data of the two poloidally separated reflectometry channels reflected at $r = 18$ cm in the core plasma. The Fourier spectrum of the first signal, the coherency spectrum of two signals and the autocorrelation function of the first one are shown for each case. Fig. 2a presents the results for the probe position at 30.5 cm. It is seen that the Fourier spectrum peak is near the zero frequency and that the autocorrelation time is 45 μs, which gives a poloidal correlation length of 5 cm at a measured velocity of 1.1×10^3 m/s. These fluctuations of the relaxation type, like 'events' observed on ASDEX [4] will be referred to as 'edge turbulence'. The additional peak at a frequency of 250 kHz is seen in the coherency spectrum. These fluctuations appear multiperiod bursts of oscillations with the zero phase difference for all of the probes. They will be referred to as 'edge quasicoherent' turbulence. The data of Fig. 2b were taken at a radius of 27.8 cm. One can see the above-mentioned 'edge turbulence' at low frequencies alongside a new type of fluctuations. It manifests itself as an increase of the high frequency tail in the Fourier spectrum with a low, but constant, coherency value. The dashed line on the coherency spectrum corresponds to the increased poloidal separation of the probes (1.2 cm). It is seen that contrary to the low frequency 'edge turbulence', the coherency of high frequencies disappears almost uniformly. The autocorrelation time of the tail is 2 μs, a poloidal correlation length is 0.29 cm and $k \times \rho_i = 0.56$. This wide frequency and low coherent type of turbulence is referred to as 'broad band' turbulence. The case of practically pure fluctuations of that type may be seen in Fig. 2d. Except for two new maxima, the Fourier spectrum is practically flat, which is characteristic of 'white noise'. The autocorrelation time is 1.65 μs, a correlation length 0.39 cm and $k \times \rho_i = 0.8$ at $T_i = T_c =$ 38 eV. The data of Fig. 2c, taken at a radius of 25.5 cm show a maximum at 40 kHz. It corresponds to the appearance of the 'quasi-coherent' bursts of oscillation with several periods at close frequencies. The wide Fourier spectral maximum results from the averaging of the bursts over time. One can see that the maximum position is shifted to 100 kHz at $r = 23.5$ (Fig. 2d), 120 kHz at the rail limiter (Fig. 2e) and 150 kHz for the core plasma (Fig. 2f). The characteristic wavelength of the bursts can be estimated from Fig. 2d to be 2.4 cm, taking into account a velocity of 2.4×10^3 m/s yielding $k \times \rho_i = 0.13$. Fig. 2d–f, also show the appearance of the forth turbulence type which corresponds to the zero frequency maximum. These fluctuations also include 'quasi-coherent' bursts component, but they contain in addition fast stochastic

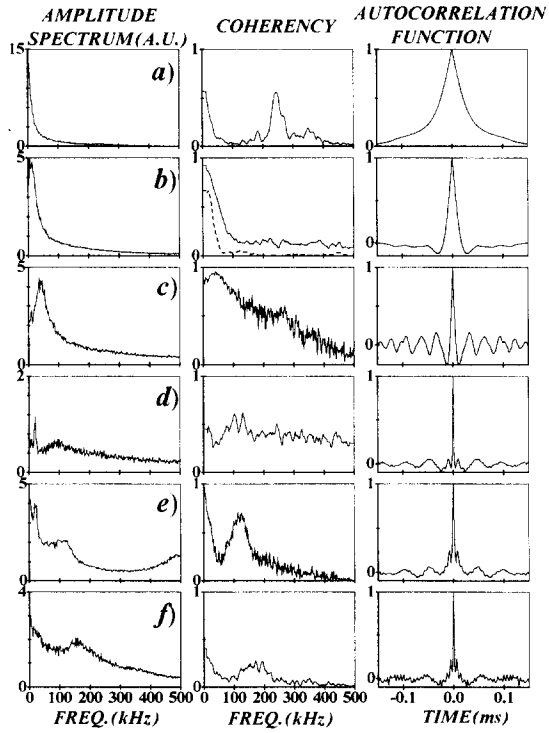

Fig. 2. Radial dependencies of the Fourier amplitude and coherence spectra and autocorrelation function. (a) Probe at $R = 30.5$ cm; (b) probe at $R = 27.8$ cm; (c) probe at $R = 25.5$ cm; (d) probe at $R = 23.5$ cm; (e) rail limiter probe; (f) correlation reflectometry at $R = 18$ cm.

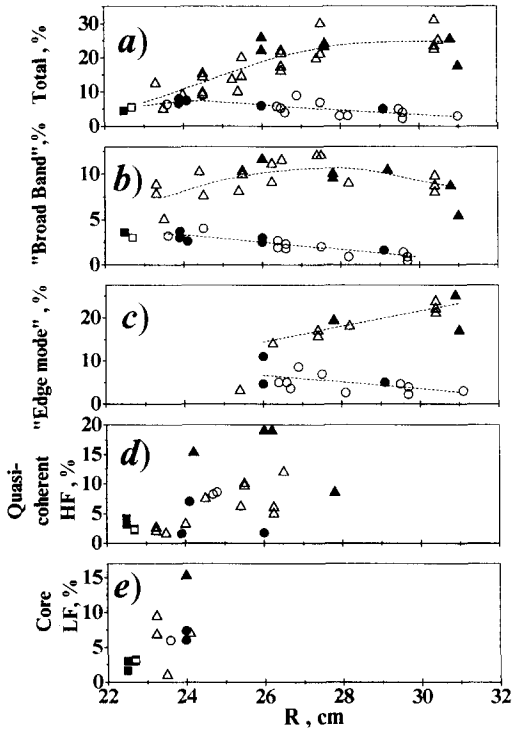

Fig. 3. Radial dependencies of the relative level of fluctuations: (a) total fluctuations; (b) 'broad band' fluctuations; (c) 'edge' fluctuations; (d) 'high frequency quasi-coherent' fluctuations; (e) 'low frequency core' fluctuations. Filled triangles – low field side probe position, ion drift down; open triangles – low field side probe position, ion drift up; filled circles – high field side probe position, ion drift down; open circles – high field side probe position, ion drift up; filled squares – rail limiter probe, ion drift down; open squares – rail limiter probe, ion drift up; dashed curves – approximation of the experimental data.

density variations similar to the 'edge' relaxation. The last three figures show that these fluctuations are typical only for the hottest SOL part and always occurs in the core plasma. So these fluctuations will be referred to as 'low frequency core' turbulence.

The radial dependence of the relative average level of ion saturation current fluctuations is presented in Fig. 3. The notations are the same as in Fig. 1. The total relative level of the fluctuations is presented in Fig. 3a. It is seen that a high asymmetry in the fluctuation level exists in the cold SOL and decreases towards the rail limiter. No difference is observed for the different drift directions. In the case of a mixture of several fluctuation types a real signal can be decomposed into its components taking into account the flat shape of the 'broad band' fluctuations Fourier spectrum in the frequency range of 0–100 kHz. The relative level of the fluctuations for the 'broad band' turbulence is presented in Fig. 3b. A high asymmetry is found in the cold plasma, but it does not disappear in the hot SOL region. The relative level of the fluctuations for the 'edge turbulence' is shown in Fig. 3c. It is also strongly asymmetric in the cold plasma. The reversal of drift direction had also no noticeable effect. It is seen that this turbulence type is limited by $r \geq 26$ cm. Thus this observation confirms the term 'edge turbulence'. The relative fluctuation levels for the high frequency 'quasi-coherent' and 'low frequency core' turbulence are presented in Fig. 3d,e, respectively. It is difficult to determine the asymmetry for those cases due to the big scatter of the points for all of four combinations. The 'high frequency quasicoherent' turbulence appears at $r = 26.5$ cm, while the 'low frequency core' turbulence appears only at $r = 24$ cm near the limiter.

The radial particle flux resulting from the turbulence is presented in Fig. 4. It was calculated as $G(r) = \langle \delta n \times \delta E \rangle / B$ from the ion saturation current δI and poloidal electric field fluctuations δE which were measured simultaneously. The brackets mean averaging over the time. The value of δE was measured by the difference in the floating potentials of two adjacent probes, neglecting temperature fluctuations. The symbols in Fig. 4 are identical to those of Fig. 3. The phase shift between the ion saturation current and electric field fluctuations always corresponds to the maximum turbulence flux. The high asymmetry is also observed between the low and high field side probe positions. A new phenomenon of the flux dependence on the variation of magnetic gradient drift direction is distinctly seen. Thus the maximum turbulent flux occurs on the low field side at a poloidal angle of about 45° in the direction of the ion drift due to the gradient of magnetic field. The maximum flux value of 1.2×10^{20} s^{-1} m^{-2} at $r = 26$ cm on the low field side corresponds to the diffusion coefficient 0.9 m^2/s which can be compared with the Bohm value of 0.35 m^2/s. The agreement is good, taking into account the high asymmetry of the turbulence flux.

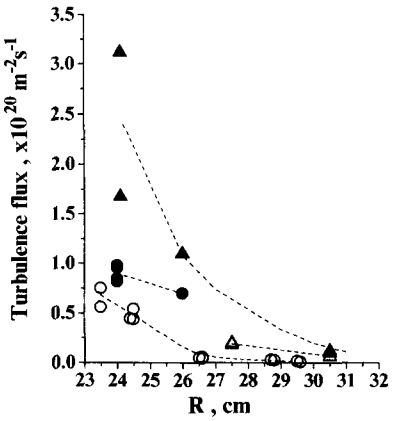

Fig. 4. Radial dependence of the turbulent particles flux. Filled triangles – low field side probe position, ion drift down; open triangles – low field side probe position, ion drift up; filled circles – high field side probe position, ion drift down; open circles – high field side probe position, ion drift up.

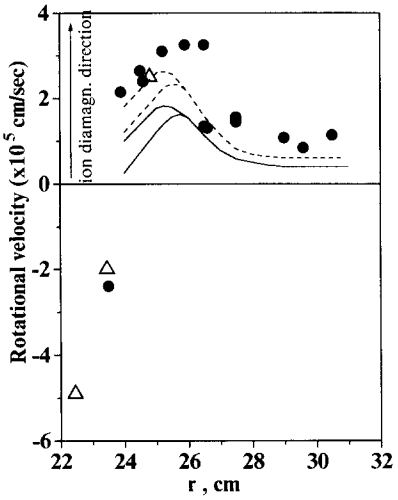

Fig. 5. Radial dependence of the rotational velocity. Open triangles – fluctuations rotation, correlation reflectometry data; filled circles – fluctuation rotation, Langmuir probes data; dashed curves – calculation of plasma rotation for $T_i = T_e$; solid curves – calculation of plasma rotation for $T_i = 2T_e$.

The observed high radial flux asymmetry proves the previous results, where ballooning plasma flows along the magnetic field lines were found [5].

The radial dependence of the rotation velocity of fluctuations, measured by the probes (circles) and correlation reflectometry (triangles) is shown in Fig. 5. The rotation of the 'broad band' is presented. The solid and dashed lines show the calculated values of the plasma rotation perpendicular to the total magnetic field for $T_i = T_e$ and $T_i = 2T_e$. The dispersion of the curves at $r \leq 26$ cm is related to the uncertainty in the floating potential presented in Fig. 1c. Perpendicular velocity was calculated according to the equation of ion radial force balance:

$$V_\perp = [V \times B]/|B| = -(\nabla P_i/(eZ_i n_i) + E_r)/B \qquad (1)$$

where n_i, eZ_i and P_i are the ion density, charge and pressure, respectively; E_r is the radial electric field. The radial electric field was calculated from the floating potential φ and T_e by the expression:

$$E_r = \delta(\varphi + \gamma T_e)/\delta r. \qquad (2)$$

The value of γ was taken from [6], where it decreases from 2.4 at $T_e = 10$ eV to 2 at $T_e = 40$ eV. It is important to note that the fluctuation rotation perpendicular to the total magnetic field was measured. Therefore, they can be compared directly with the calculations. It is seen from Fig. 5, that all of the points for the fluctuation rotation are higher than both calculated curves. It means that the fluctuations may additionally rotate with respect to the plasma in the ion diamagnetic drift direction. Therefore, they have an ion, rather then electron nature. It must be noted that there is a good agreement between the velocities measured with probes and correlation reflectometry. Both diagnostics show the rotation reversal at $r = 24$ cm.

The relative level of the floating potential fluctuations is in factor 1.7 higher then the relative ion current fluctuations for 'edge' and 'broad band' turbulence, while Boltzmann relation $\delta I/I \approx (e * \delta\varphi)/T_e$ holds for 'quasi-coherent' fluctuations.

4. Discussion and conclusions

The presented results show, that all of three turbulence types previously identified with correlation reflectometry in the core plasma were observed in the SOL by means of Langmuir probes. In addition, two specific 'edge' turbulence types were found. The main SOL parameters were symmetrical within the scatter of the experimental points.

The 'edge quasi-coherent' turbulence is similar to the edge localized $n = 0$ mode in the Alfven frequency range identified on TFTR [7]. It has maximal amplitude and frequency 500 kHz at the rail limiter as it is seen in Fig. 2e.

The 'edge' turbulence is characterized by spatially long relaxation bursts of the dimensions about 3–5 cm with $k \times \rho_i = 0.03$. It exists in the cold SOL regions and is highly asymmetric poloidally. The possible physical mechanism was discussed in [8], where the comparison with the resistive drift ballooning instability was presented. Unfortunately, this theory failed to explain the small rising time. Moreover, the magnetic shear was not considered.

The 'broad band' turbulence was found to be the most universal instability, as it exists over the whole plasma column. It is characterized by a very broad and practically constant amplitude Fourier and coherency spectra. The value of coherency is, as a rule, small. The autocorrelation time is about 2 μs, corresponding to spatial dimensions of 0.6–0.25 cm and $k \times \rho_i = 0.5$–0.8 for $T_i = T_e$ and 0.7–1.1 for $T_i = 2T_e$. This turbulence is also highly asymmetric poloidally. The 'broad band' have additional rotation in the ion diamagnetic drift direction with respect to the plasma, thus indicating its possible ion origin. The ITG instability is considered now, as the physical mechanism of the 'broad band' turbulence.

The origin of the two types of highly correlated poloidally turbulence observed is not clear now. However, they resemble those revealed long time ago by visual imaging of the plasma [9–11]. Some indications on possible physics were made in [1], where the high frequency mode was associated with an 'impurity driven' turbulence, while the low frequency mode was considered as the turbulence driven by the main ions.

The turbulent fluxes were found to be highly asymmetric, with their maximum shifted poloidally in the ion gradient drift direction.

Acknowledgements

The authors wish to acknowledge the support of T-10 diagnostic and operational staff. This work was supported by Russian Foundation for Fundamental Researches, Grants Nos. 94-02-06521-a and 96-02-18807.

References

[1] V. Vershkov, 22th EPS Conf., Bournemouth 1995, Vol. 19C, Part IV, p. 5.
[2] V. Vershkov et al., Proc. of IAEA Conf. Seville 1994, Plasma Phys. Controlled Nucl. Fusion 2 (1995) 65.
[3] V.A. Vershkov et al., 21th EPS Conf. Montpellier 1994, Vol. 18B, Part 3, p. 1192.
[4] M. Endler and L. Giannone, 20th Eur. Conf. Lisbon 1993, Vol. 17C, Part 2, pp. 583–586.
[5] A.V. Chankin et al., J. Nucl. Mater. 145–147 (1987) 789.
[6] G.F. Matthews et al., J. Nucl. Mater. 145–147 (1987) 225–230.
[7] Z. Chang et al., Nucl. Fusion 35 (1995) 1469–1479.
[8] V.A. Vershkov et al., 21th EPS Conf. Montpellier 1994, Vol. 18B, Part 2, p. 886.
[9] N.D. Vinogradova and K.A. Razumova, Proc. of IAEA Conf. 1965, Plasma Phys. Controlled Nucl. Fusion 2 (1966) 617.
[10] D.H.J. Goodall, J. Nucl. Mater. 111–112 (1982) 11.
[11] S.J. Zweben and S.S. Medlley, Phys. Fluids B 1 (1989) 2058.